Depth profile of thin coating through surface and interfacial cutting analysis of UV curing system

Ji-Won Park [a,b], Kyeng-Bo Sim [a], Gyu-Seong Shim [a], Jong-Ho Back [a], Dooyoung Baek [a,b], Hyun-Joong Kim [a,b,*], Seunghan Shin [c]

[a] Laboratory of Adhesion and Bio-Composites, Seoul National University, Seoul 08826, Republic of Korea
[b] Research Institute of Agriculture and Life Sciences, College of Agriculture and Life Sciences, Seoul National University, Seoul 08826, Republic of Korea
[c] Green Process R&D Department, Korea Institute of Industrial Technology, Cheonan-si, Chungnam 31056, Republic of Korea

HIGHLIGHTS

- The curing properties of an ultraviolet ray thin coating system were analyzed using a slide cutting system
- This is the first study evaluating the curing properties of a coating material using the resistance of the blade.
- Depending on the reaction conditions, it has oxygen inhibition effect up to 15um from the surface.
- As the concentration of functional group and initiator increases, the surface uncured zone thickness decreases.

GRAPHICAL ABSTRACT
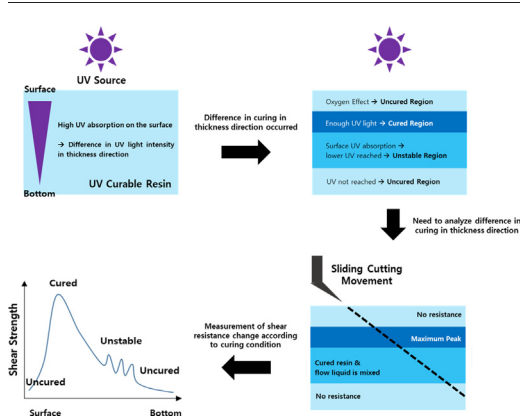
ARTICLE INFO

ABSTRACT

There are various thin coating technologies, among which the UV coating technology is attracting attention in next-generation industries. In order to utilize the UV coating system stably, it is necessary to analyze and address the problems of surface oxygen inhibition and UV penetration, which lead to irregular curing characteristics. For this, three different UV-curing resins were selected. The effects of the structural difference of the material and change in the initiator content along the thickness direction during UV curing were evaluated by the sliding cutting technique (which involves cutting the coated surface at a superfine angle). Thus, it was confirmed that the effect of surface oxygen inhibition during UV curing is very large on the surface. Here, surface curing could be induced by increasing the functional group concentration and introducing a hybrid curing system. With increasing initiator content, the formation of a material with a high curing density on the surface and an irregular hardening structure in the deep part was confirmed. Therefore, the sliding cutting technique is a very effective approach to control the thickness profile of a UV coating system.

* Corresponding author at: The Lab of Adhesion and Bio-Composite, Program in Environmental Materials Science, Department of Forest Science, Seoul National University, Seoul 08826, Republic of Korea.
E-mail address: hjokim@snu.ac.kr (H.-J. Kim).

1. Introduction

Thin coating technology has traditionally been employed for system protection and the surface modification of materials. Its usage has recently gradually expanded to key areas such as biomedical/next-generation electric and electronic fields [1,2]. Thin coatings range in size from tens of micrometers to tens of nanometers. Thin coating technology can prevent oxidation of the material and enhance the biocompatibility of the material while maintaining the appearance and surface reactivity of the raw material [3,4].

Sputtering, electron beam, chemical vapor deposition (CVD), wet coating, electrochemical/chemical coatings, and UV coating techniques are employed to prepare thin coatings. Each method has its own advantages depending on the raw material and shape of the coating layer. Among them, the UV coating technology is suitable to protect/primer coatings of tens of micrometers. UV curing is a process that transforms a functional monomer into a cross-linked polymer by a reactive radical initiated by free radicals or ions. UV coating technology is regarded as eco-friendly process, because it is simple, energy-efficient, and very fast compared to other technologies. However, the toxicity and stability of the material itself are still under study, and migration or remaining an issue to be resolved [5–7].

Nevertheless, some drawbacks need to be addressed to continuously expand the utilization of UV coating technology to next-generation industries. Free radical technology is most commonly used in UV coatings. When using a free radical system in UV coating technology, the inhibition of the reaction by oxygen on the surface, UV transmission by surface absorption, and the problem of the uncured bottom site are key issues that require solutions [8,9]. Typically, to resolve such issues, the system is designed such that the surface state can be purged with nitrogen or irradiated with excess UV to reach the deep part; however, such solutions are not suitable under space limitations and high-speed process systems [10,11].

In order to analyze the curing characteristics of a UV curing system based on free radicals, Raman analysis or image-Fourier-transform infrared spectroscopy (FTIR) have been employed. However, these approaches have limited efficiency. It takes a long time to analyze one system or prepare a specimen. Uncured specimens cannot be individually sampled, making accurate measurement difficult [12]. Typical evaluations such as those of UV light transmission characteristics, reaction transfer rate, or shrinkage rate are suitable to analyze thick films, but are difficult to achieve in thin coatings. As the existing test method involves using bulk materials or a mass-based evaluation, it is difficult to apply it to the analysis of the curing characteristics of thin films [8,13].

The components of the UV curing system are varied. These factors can be varied to control the reactivity of the UV curing system [14,15]. The curing characteristics with respect to the thickness direction are changed according to the reactive control. This is because the transmittance and partial curing of UV are changed. Variable control of the

material is easy, but changes in the curing properties are also rapid. Therefore, a system capable of quickly analyzing various controllable variables is required [16,17].

The sliding cutting technique involves cutting thin materials from the surface of the specimen to a deep portion at a very minute inclination angle [18]. The inclination angle is determined by the velocity ratio between the horizontal direction and vertical direction. This technique has been utilized to fabricate microsized test specimens for the surface oxidation of materials or to measure the adhesion of thin-film coating layers of ion batteries. When the cutter moves to the deep part, the change in the curing degree causes a change in the shear resistance applied to the cutter. In the past, this has been utilized to confirm the interface between multilayer thin films [19,20]. Although the sliding cutting technique has been used for sampling or interfacial peel strength measurement, no research has been conducted to analyze the characteristics of materials directly using shear resistance. In particular, this research method is an approach to observe bulk properties of materials. It is a new test method that can directly observe the physical properties of materials which change according to the curing properties.

In this study, the curing depth profile of a thin coating film was analyzed through the micro strength changes during sliding cutting; moreover, surface curing inhibition and deep penetration analyses of the UV coating system were performed. Finally, the influence of the composition of the material on the thickness direction in the curing profiles was analyzed.

2. Experimental

2.1. Surface and interfacial cutting analysis system

The surface and interfacial cutting analysis system (SAICAS, Daipla Wintes, Japan) is a machine for slicing thin specimens from the surface to the interface using sharp diamond cutting blades. Fig. 1 is a schematic diagram of the SAICAS, where "step 1" measures the shear strength of the material and "step 2" measures the peel strength at the interface. Thus, SAICAS can perform two major measurements; however, this study focuses on step 1. The movement of the diamond cutter was controlled to be 50 μm/s horizontally and 0.5 μm/s vertically, with a cutting slope progression to 0.57°. The cutting surface of each specimen is shown in Fig. 2. The larger the aspect ratio, the higher the resolution of the depth profile. However, the viscoelastic nature of the coated surface causes issues with the restoration of pressure. Therefore, we adjusted the aspect ratio from 10 times to 1000 times, and after pre-evaluation, decided the best ratio for this experiment.

2.2. Composition of materials

The UV coating system consisted of a multifunctional oligomer capable of forming a cross-linked structure, reactive diluent for
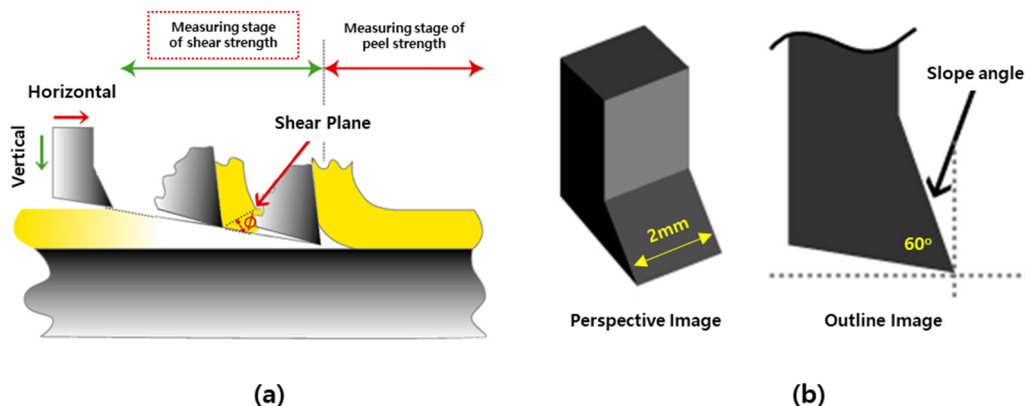
Fig. 1. (a) Schematic diagram of the SAICAS test [21] (b) shape of cutting blade.
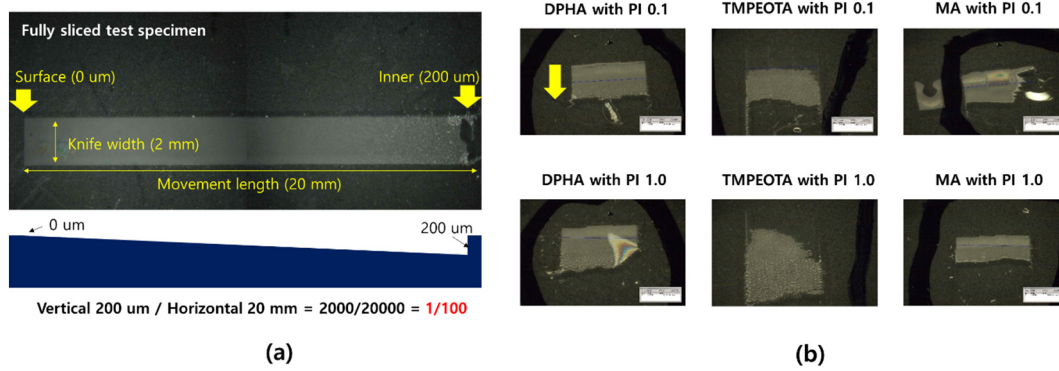
Fig. 2. (a) Sliding cutting test piece (movement ratio, 1:100; slope, 0.57°) obtained with SAICAS (b) post-cut image by each specimen.

controlling the viscosity and reactivity, an additive for controlling the functionality, and a photoinitiator [22]. Among them, the multifunctional oligomer has a high functional group density and directly forms a three-dimensional cross-linked structure, which has the greatest influence on the reactivity and coating film performance. In this study, we investigated the curing characteristics of three multifunctional oligomers, dipentaerythritol hexa acrylate (DPHA, Sartomer, France), trimethylolpropane ethoxylate triacrylate (TMPEOTA, Sartomer, Rieux, France), and melamine acrylate (MA, Miwon Specialty Chemical, Republic of Korea) (Table 1).

DPHA is a hexafunctional material with a very high functional group density and high reaction rate. TMPEOTA, which has a low functional group density and high structural flexibility, was selected based on DPHA, and MA, which can be cured by thermal hybridization, was selected to showcase a complementary technology to the single UV curing system. 1,2-octanedione, 1-[4-(phenylthio) phenyl]-,2-(O-benzyloxime) (PI, CIBA, Germany) was used as the photoinitiator. The photoinitiator was prepared as 0.1/1.0 parts per hundred resin (phr) of the oligomer. The coating thickness was 100 μm ± 5 μm, which was controlled by blade coating. In order to increase the wettability and adhesion of the oligomers and counter the issue of UV reflection, we applied a coating to the slide glass. The UV curing equipment utilized a 250 W class metal halide lamp. The UV transmittance (D_{dp}) was determined by the total energy delivered to the system, the initiator content, and critical E of the system (ε), which can be interpreted as [8]:

$$D_{dp} \Leftrightarrow \frac{2}{2.303\epsilon[PI]} \tag{1}$$

In this system, we tried to observe the change in UV transmittance with the change in the initiator content by maintaining the UV dose constant. The UV light source was a metal lamp, irradiated with 50 mJ/cm^2 UV on the surface, and cured in a normal atmospheric environment. MA was additionally thermally cured at 80 °C for 30 min to induce curing by heat.

3. Result & discussion

3.1. Curing depth profiling according to structural characteristics of the material

Fig. 3 shows the results for the sliding cutting measurements of DPHA (PI 0.1 phr). Both, the horizontal and vertical strengths, have maximum values at 1 to 2 μm from the surface, which is attributed to the fracture resistance of the cured surface. Oxygen inhibition is known to significantly affect the surface in a UV coating system [23]. In the experimental results, the hardest layer (of high hardening density) is formed on the surface. After activation of the initiator on the surface of the UV coating system, there occurs a competitive reaction of curing with acrylate or inhibiting with oxygen. It is generally known that the reaction rate of acrylate tends to be proportional to the functional group. Park et al. reported that the reactivity of acrylates varies with the reaction environment but tends to be proportional to the functional groups [8,22]. When a high-density acrylate such as DPHA is used, the curing reaction of the acrylate is predominant. In a multifunctional acrylate structure, two or more functional groups must react to form a three-dimensional cross-linked structure. As DPHA has a six-functional structure, the crosslinking reaction is advantageous, because only one-third of the functional groups participating in the reaction form a three-dimensional cross-linked structure. The vertical strength gradually decreases and becomes negative from 4 to 5 μm because of the elastic characteristics of the cured film, and the compression energy in the vertical direction during cutting affects that in the horizontal direction. The recovery characteristic from the upper part to the lower part of the cutting blade was obtained in order to reverse the direction of the force.

Further, it can be assumed that the test specimen generated on the cut surface continuously interacts with the cutting knife. The horizontal strength is measured to be stable until 12.5 μm and tends to oscillate thereafter. The vibration phenomenon is due to random energy transfer from irregular cracks. This is attributed to the weak internal cohesion of the material with a low degree of curing. Thereafter, the horizontal strength decreases abruptly and the vertical strength is partially recovered at 18 μm. Subsequently, the coating layer gets peeled from the surface, owing to incomplete curing.

Table 1
Key properties of multifunctional oligomers.

Materials	Dipentaerythritol hexa acrylate (DPHA)	Trimethylolpropane ethoxylate triacrylate (TMPEOTA)	Melamine acrylate (MA)
Functionality number	6	3	3
Molecular weight (g/mol)	524	692	~1500
Average functionality number (mol/g)	0.0114	0.0043	0.002
Curing type	UV (radical)	UV (radical)	UV (radical)
			Thermal (condensation)
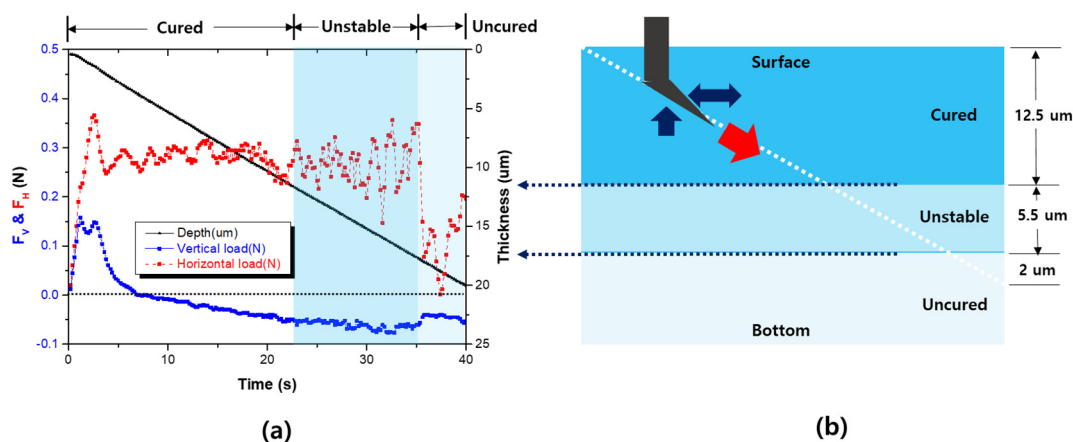
Fig. 3. Sliding cutting strength using DPHA (PI 0.1 phr) (a) experimental results (b) interlayer classification by degree of curing.

In the uncured region, the phase of the material completely changes, from a solid phase with a viscoelastic characteristic to a viscous liquid phase. The strength tends to change abruptly as peeling occurs at the boundary between the unstable region and uncured region. In the horizontal section, the strength suddenly decreases, while in the vertical direction, it tends to suddenly increase as the pressure for vertical pressing disappears owing to the elasticity of the material.

Fig. 4 shows the results of the sliding cutting measurements of TMPEOTA (PI 0.1 phr). In TMPEOTA, the knife moved about 2.5 times deeper than in DPHA. This is attributed to uncured portions on the surface. The stress changed only slightly for both vertical and horizontal strengths up to 15.1 μm. The cured form (Fig. 6) obtained after cutting the non-cured layer on the surface shows that while some viscous oligomers are cut, fluidity still remains. This occurs because oxygen in the atmosphere penetrates the surface of the coating owing to the oxygen inhibition effect on the surface. Oxygen acts as a very strong inhibitor to capture and remove radicals during radical formation and polymer growth. Therefore, it is considered that such an oxygen interference effect results in an uncured characteristic on the surface. The functional density of TMPEOTA is 38% of that of DPHA. After the radicals are formed, there is high probability that the inhibiting reaction by oxygen is more dominant [22,24].

In addition, as the number of functional groups is 3, it is necessary to process a reaction stochastically five times or more in order to construct a three-dimensional network having the same crosslink density as DPHA. For highly flexible materials such as TMPEOTA, the total reaction rate is known to be higher than for materials such as DPHA [14], assuming that sufficient energy and initiator are provided. In a curing system

with a certain amount of light, a material having a high functional group density such as DPHA is more advantageous for curing. Subsequently, the horizontal strength tends to increase continuously up to 30 μm. TMPEOTA tends to increase in intensity toward the deep part, while DPHA has a peak at the surface, since it is less affected by oxygen inhibition toward the deep part. Thereafter, the horizontal strength tends to oscillate, because the cured structure becomes unstable.

Fig. 5 shows the sliding cutting measurement results of MA (PI 0.1 phr). MA has a lower functional density than TMPEOTA. Uncured sections are observed due to the oxygen inhibition effect on the surface, but both the vertical load and horizontal load tend to increase rapidly from 2 μm. The section up to 7.1 μm is defined as a mixed zone, in which the acrylate was partially cured by UV. The partially cured state still possesses fluidity. However, the partially cured oligomer is additionally cross-linked by thermosetting to begin forming a three-dimensional cross-linked structure. Therefore, the mixed section, where the UV curing structure and thermosetting structure are crossed, is formed by UV and thermal curing. The thermal curing system of MA can be realized by its own structure without additional additives, and is known to be very effective for forming three-dimensional structures [25].

After 7.1 μm, the horizontal resistance shows a tendency to decrease while oscillating, while the vertical resistance tends to decrease sharply. The oscillation of the horizontal resistance is due to the continuous deformation and breakage of the material. The degree of curing decreases and the overall tendency of the resistance to decrease. It can be said that the decrease in vertical resistance is affected by the viscoelastic tendency, similar to that for other test specimens. Therefore, at this point,
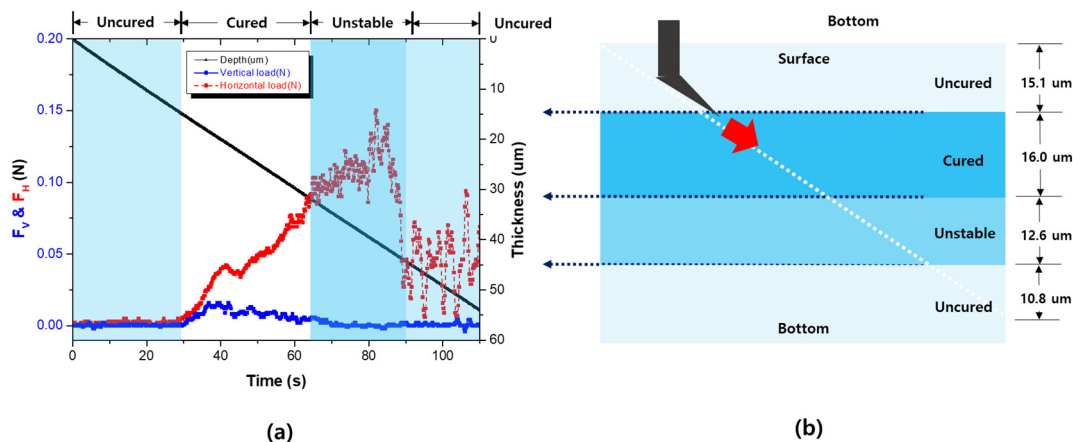
Fig. 4. Sliding cutting strength using TMPEOTA (PI 0.1 phr) (a) experimental results (b) interlayer classification by degree of curing.
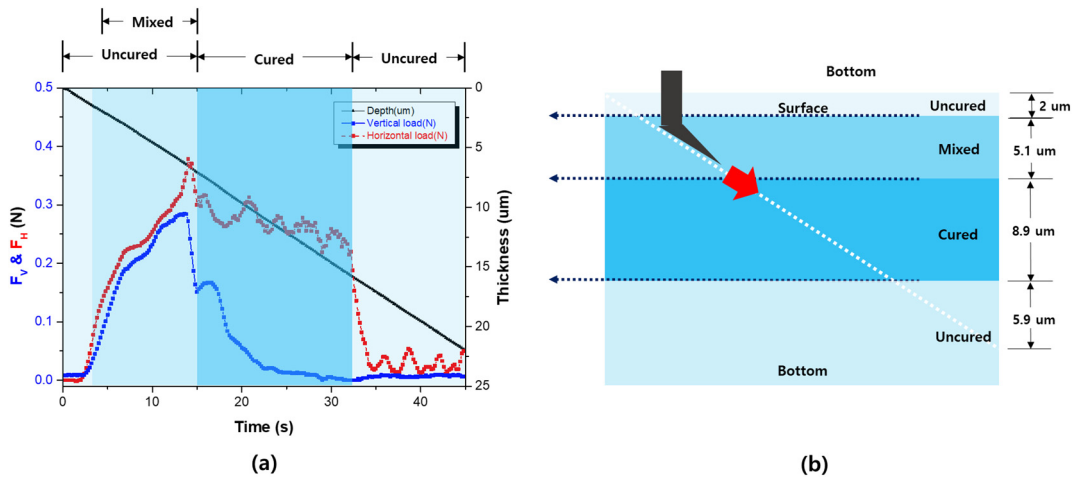
Fig. 5. Sliding cutting strength using MA (PI 0.1 phr) (a) experimental results (b) interlayer classification by degree of curing.

additional curing may have taken place by the heat after sufficient three-dimensional crosslinking by UV. After 16 μm, the horizontal strength tends to decrease rapidly, but unstable sections are not found; this is attributed to hardening by thermal curing. As shown in Fig. 8, the film is cut in a certain shape from the initial stage to the deep portion. It can be confirmed that film breakage occurs at a point where the curing density is weakened.

Fig. 6 shows the surface cutting process each materials with PI 0.1 phr. At Fig. 6a, it can be confirmed that the film is initially cut in thin film form, and then tends to move upward along the cutter face. Further, the fracture surface becomes rough with deeper cutting, which is attributed to irregular cracks generated by formation of the abovementioned uncured portion. Finally, the cured film gets peeled off from the surface of the adherend, resulting in total breakdown.

When the opposite surface is exposed to UV, there is a limit to which the UV can reach. This serves as a factor for forming an uncured layer between the coating layer and adherend; it can be said that the fracture was formed at the weakened point. In order for the coating material to strongly adhere to the surface, wetting and physical/chemical/electrical coupling between the coating material and adherend surface are required [26]. Thereafter, sufficient cohesion is required to transfer the bonding energy to the coating material. If adequate UV does not reach the interface, the degree of curing will be low, and consequently, a dense polymer network will not be formed. Finally, as the cohesion weakens, adherent peeling occurs.

Fig. 6b shows that the gel film is peeled off, due to the complete mixture of the cured structure and non-cured structure. At 43.7 μm, the horizontal strength decreases sharply, due to the film breakdown that
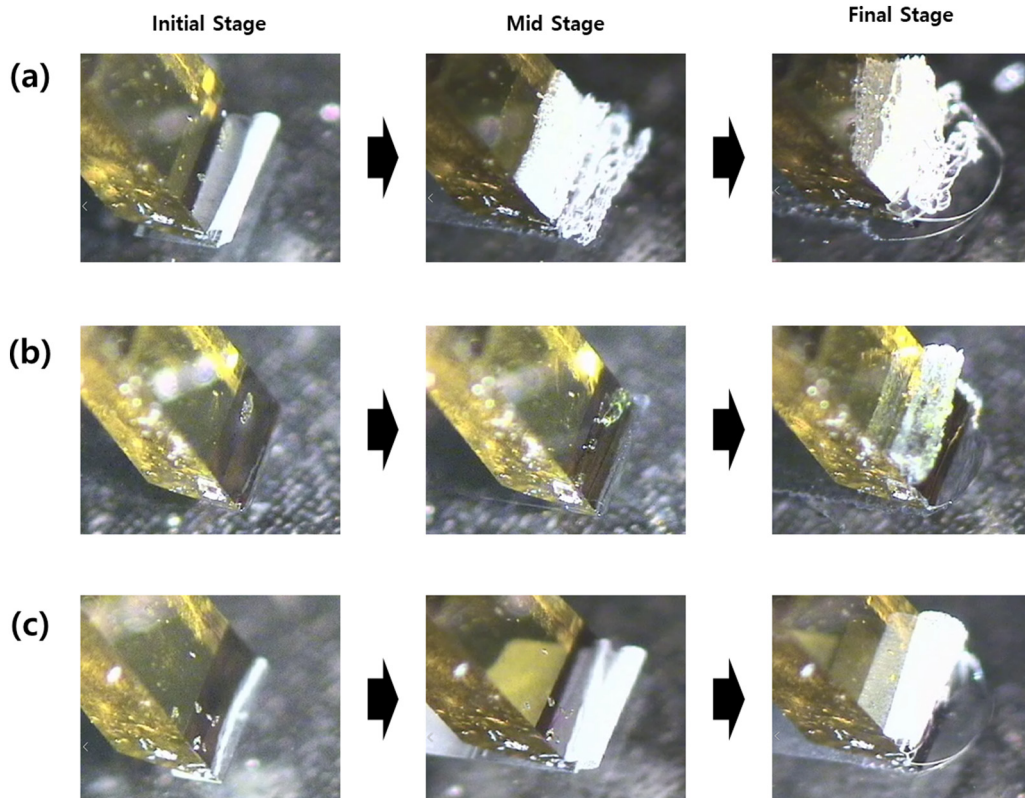
Fig. 6. Surface cutting process of each materials with PI 0.1 phr (a) DPHA (b) TMPEOTA (c) MA.
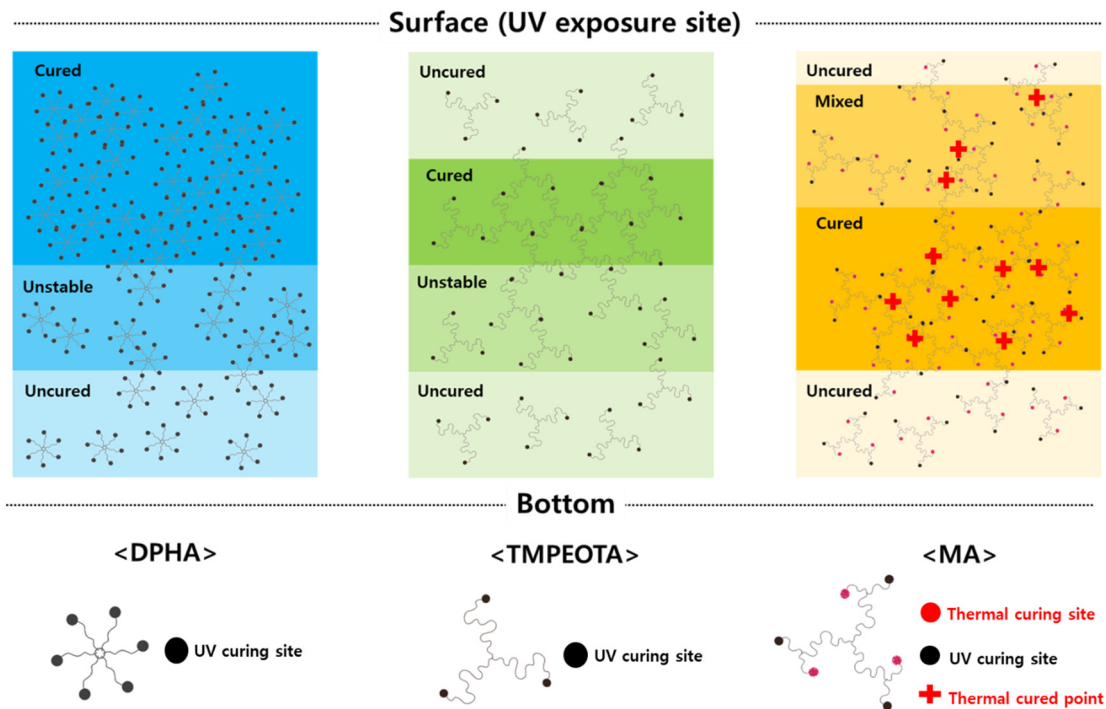
Fig. 7. Difference in curing characteristics of the three different materials in the thickness direction.

occurs as the uncured region increases. The horizontal strength of TMPEOTA (maximum 0.15 N) is half that of DPHA (maximum 0.35 N), due to failure to form a dense cured structure as a whole. Peeling occurs at more than twice the depth in TMPEOTA than in DPHA, due to cohesion of the cured layer established by each material, rather than the difference in the UV arrival depth. As the blade progresses in cutting, shear strength is generated, which is affected by the cohesion of the layer. As curing progresses, the brittle characteristics are strengthened and the probability of crack propagation increases during cutting. Therefore, for TMPEOTA with a low curing density, the knife can be moved more stably and deeply [27]. The difference in the characteristics of the mixed section and cured section can be possibly attributed to the phase difference between the two sections. As curing progresses, the state changes to liquid ➔ semi-solid ➔ solid. In the semi-solid section, the material is compressed rather than "destroyed". As curing progresses, the resin changes to a solid state with brittle characteristics, which affects the vibration characteristics mentioned above.

The three different materials have completely different curing properties from the surface to the depth. Fig. 7 shows the curing structure of the three materials from the surface to the depth, highlighting the difference in the curing density depending on the structural characteristics of the material. TMPEOTA and MA, which have a relatively low acrylate concentration, exhibit an uncured surface due to oxygen inhibition. However, in the case of MA, oxygen inhibition is complemented by thermosetting, resulting in a section exhibiting two types of curing from the surface. Completely different curing characteristics are exhibited in the thickness direction according to the structural difference of each material and complementary curing methods.

3.2. Curing depth profiling according to initiator content

Fig. 8 shows the difference in the curing behavior of DPHA for different initiator contents. There is a section where the strength increases rapidly at the surface, following which the vertical load shows a sharp
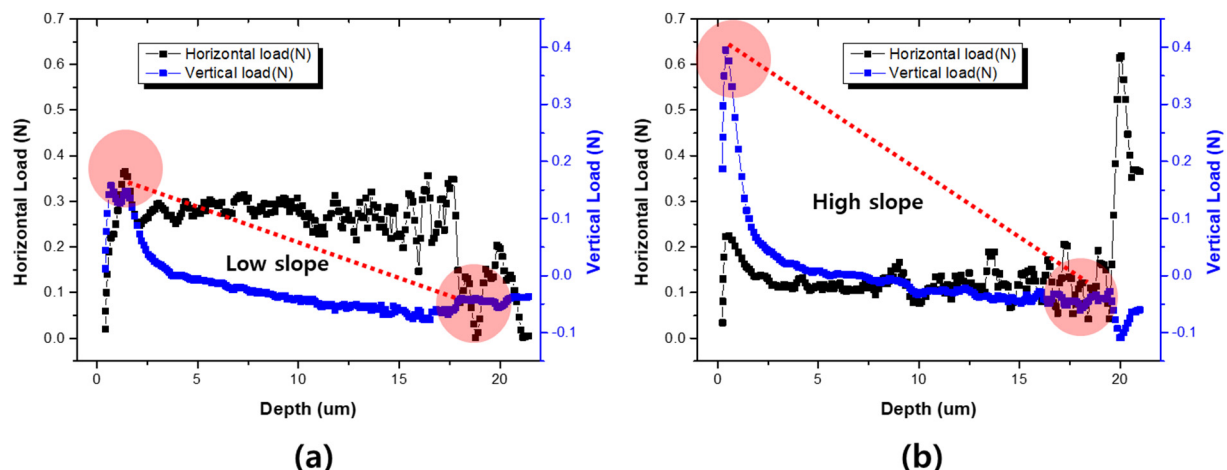
Fig. 8. Comparison of sliding cutting characteristics of DPHA according to initiator content (a) 0.1 phr (b) 1.0 phr.
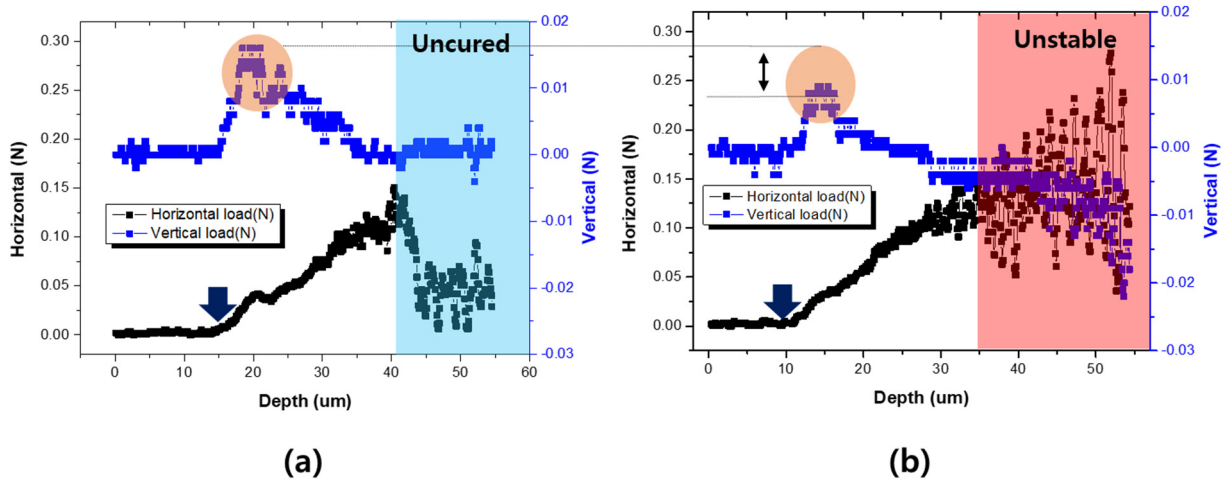
Fig. 9. Comparison of sliding cutting characteristics of TMPEOTA according to initiator content (a) 0.1 phr (b) 1.0 phr.

decrease characteristic, and the horizontal load tendency tends to be more frequent, but the characteristic shows a similar tendency in that the strength changes during a certain period. When the content of the initiator is 1.0 phr (Fig. 8b), however, the maximum vertical load at the surface is about 2.13 times that in the case of 0.1 phr (Fig. 8-a), and load reduction occurs very rapidly. This is attributed to the absorption of UV and initiation reaction increase at the surface with increasing initiator content, thereby resulting in a rapid increase in the curing density at the surface.

Fig. 8 shows that the cutting process of DPHA (PI 1.0 phr) results in the formation of flakes during surface cutting, unlike the preceding 0.1 phr condition (Figs. 3 and 6); this material exhibits high hardness, but is brittle during curing. The negative load also decreases with the brittleness. As the cutting surface approaches the deep part, the film falls off its attachment, causing the surface to break. Both samples exhibit completely different fracture tendencies in the uncured sections. As the blade progresses with constant resistance, it will encounter other conditions in the uncured section. For 0.1 phr, the layer of the less-crosslinked surface is separated and the horizontal resistance rapidly disappears. On the other hand, For 1.0 phr PI in which the crosslinking density is increased due to the high content of the initiator, the blade is affected by the hardened surface layer, and the strength tends to increase sharply. The tendency of change of strength in this section is irregular rather than constant according to the degree of curing;

hence, this characteristic can define the characteristic of the uncured section.

With increasing initiator content, the section where the horizontal strength increases is advanced. This is attributed to an increase in the range over which the oxygen inhibition effect can be overcome as the reactivity of the initiator increases, as with DPHA. As the initiator content increases, the transmittance of UV to the deep part decreases; therefore, the horizontal load tends to oscillate rapidly from about 35 μm and the vertical load begins to generate negative pressure. The amount of UV reaching the deep part gradually decreases from the surface. Therefore, the inner site is cured to a lower extent than the surface. However, as the content of the initiator increases, there is a higher probability for the formation of a crosslinked structure due to an increase in the relative site of reaction. Therefore, when the content of the initiator is high, a cured, non-cured mixed structure is formed at the core portion and oscillation occurs.

Fig. 9 shows the cutting profile of TMPEOTA (PI 1.0 phr). Unlike the previous 0.1 phr test specimen, the profile is wavy on the cutting surface. When the initiator content is low, a uniform film-like structure with a sufficient curing density is formed in a certain section. On the other hand, when the initiator content is high, an irregular curing structure and a highly viscous elastic body are formed. In the deeper part, a rough structure is formed by non-curing, which causes energy to be absorbed, contracted, and then sent out again during the movement of
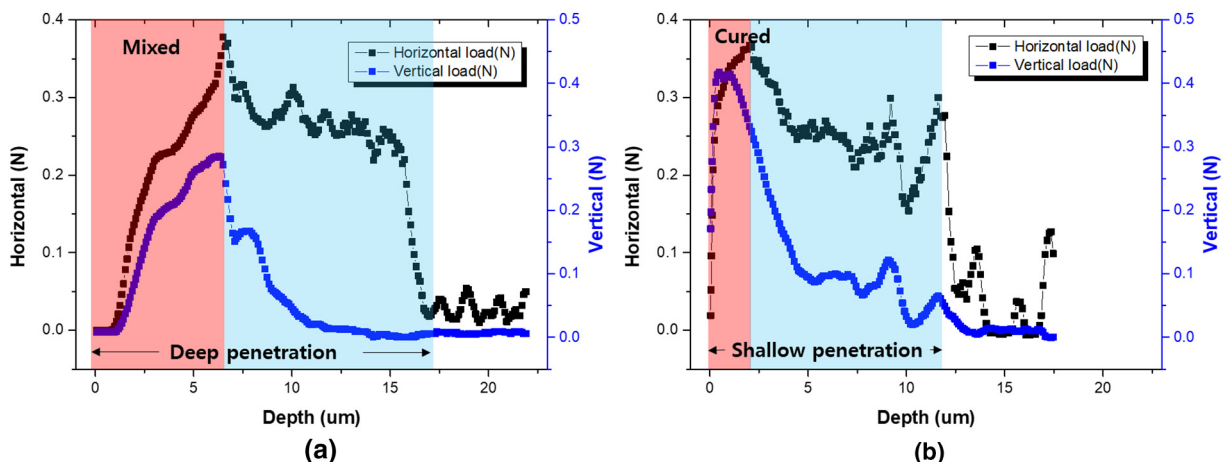
Fig. 10. Comparison of sliding cutting characteristics of MA according to initiator content (a) 0.1 phr (b) 1.0 phr.
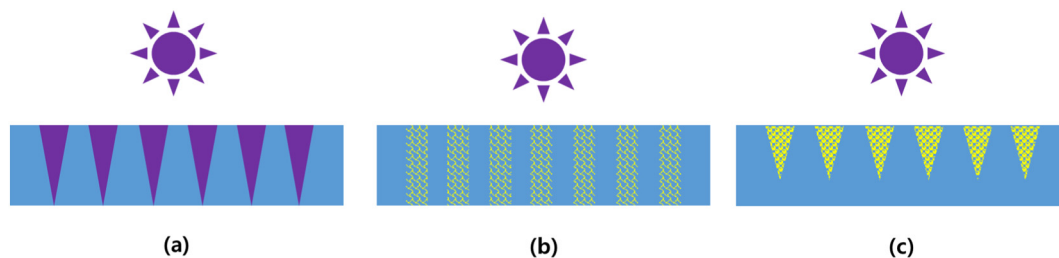
Fig. 11. Change in light transmittance according to initiator content. (a) Typical light transmission (b) low initiator content (c) high initiator content.

the cutter. Similar tendencies are seen when cutting materials such as rubber.

Fig. 10 shows the difference in the curing behavior of MA for different initiator contents. When the initiator content is increased, it is confirmed that a mixed zone is not formed, whereas a strong curing layer is formed on the surface; this is similar to that observed for DPHA. Thus, a high curing density is obtained by additional thermal curing in a state where a relatively high density of the UV curing structure is formed on the surface. Moreover, with increasing initiator content, the section where the strength decreases is also narrowed.

MA is similar to DPHA, fragmented fracture occurs, but there is a difference in shape. The molecular weight of MA is much larger than that of DPHA; further, owing to the high flexibility of the structure, a relatively soft film is formed after curing. Therefore, the cut pieces exhibit an acicular or particle structure instead of powder. Hybrid specimens cured with UV and heat have a very high cross-linking density, are fragile, and most energy-transferable. Therefore, peeling occurs most rapidly.

Fig. 11 shows the effect of initiator content on curing. UV is generally absorbed from the surface, and the absorption tends to decrease gradually toward the depth. As the initiator content decreases, the cured density decreases as a whole, but light transmission increases. On the other hand, when the initiator content increases, a curing layer with a high density on the surface is formed, but the light transmittance is drastically reduced.

4. Conclusion

The curing properties of a UV coating system in the thickness direction were evaluated using the sliding cutting technique. The curing structure plays a major role in changing the shear strength of the material, which was evaluated by a slide cutting strength measurement method. During UV curing, the surface oxygen inhibition effect was very pronounced at around 10 μm on the surface. In this case, surface curing could be induced by increasing the functional group concentration. Further, by introducing a hybrid curing system, it was possible to reduce the uncured section and increase the overall degree of curing. As the initiator content increased, the transmission of UV decreased, and thus, a high curing density on the surface and an irregular curing structure in the deep part were obtained. Control of the initiator content was effective in supplementing the surface oxygen inhibition effect in UV coating; however, an increase in the amount used could act as a negative factor in curing of the deep area. Therefore, the composition must change as the coating thickness changes. If the coating is thin and UV penetration is not an issue, changing the initiator content is the most efficient approach. However, if the coating is thick, it would be effective to introduce a method that can complement UV curing, such as a hybrid curing system. Through this study, it was confirmed that the curing characteristics of UV curable materials can be measured in a bulk state. This method is a very fast measurement method, and it is judged that it is a technique to evaluate the curing characteristics changing according to the UV process variable which can be varied in the laboratory or the field in real time. This technology can be applied not only to UV coating, but also to 3D printing, dental materials, and so on.

CRediT authorship contribution statement

Ji-Won Park: Conceptualization, Data curation, Methodology, Writing - original draft. **Kyeng-Bo Sim:** Formal analysis, Resources, Validation. **Gyu-Seong Shim:** Formal analysis. **Jong-Ho Back:** Data curation. **Dooyoung Baek:** Data curation. **Hyun-Joong Kim:** Funding acquisition, Writing - review & editing. **Seunghan Shin:** Funding acquisition, Project administration.

Acknowledgement

Appendix A. Supplementary data

Supplementary data to this article can be found online at https://doi.org/10.1016/j.matdes.2019.107855.

References

[1] M. Cano, R. Núñez-Lozano, R. Lumbreras, V. González-Rodríguez, A. Delgado-García, J.M. Jiménez-Hoyuela, G. de la Cueva-Méndez, Partial PEGylation of superparamagnetic iron oxide nanoparticles thinly coated with amine-silane as a source of ultrastable tunable nanosystems for biomedical applications, Nanoscale 9 (2) (2017) 812–822.
[2] L. Marasinghe, C. Croutxé-Barghorn, X. Allonas, A. Criqui, Effect of reactive monomers on polymer structure and abrasion resistance of UV cured thin films, Prog. Org. Coat. 118 (2018) 22–29.
[3] E. Reedy, Thin-coating contact mechanics with adhesion, J. Mater. Res. 21 (10) (2006) 2660–2668.
[4] Y. Li, I.-S. Lee, F.-Z. Cui, S.-H. Choi, The biocompatibility of nanostructured calcium phosphate coated on micro-arc oxidized titanium, Biomaterials 29 (13) (2008) 2025–2032.
[5] X. Guo, R. Li, Y. Teng, P. Cao, X.A. Wang, F. Ji, Effects of surface treatment on the properties of UV coating, Wood Res. 60 (4) (2015) 629–638.
[6] B. Curatolo, UV technology for protection of surfaces, UV EB Technol. (2015) 22–29.
[7] Y. Li, H. Shao, P. Lv, C. Tang, Z. He, Y. Zhou, M. Shuai, J. Mei, W.-M. Lau, Fast preparation of mechanically stable superhydrophobic surface by UV cross-linking of coating onto oxygen-inhibited layer of substrate, Chem. Eng. J. 338 (2018) 440–449.
[8] J.-W. Park, G.-S. Shim, J.-H. Back, H.-J. Kim, S. Shin, T.-S. Hwang, Characteristic shrinkage evaluation of photocurable materials, Polym. Test. 56 (2016) 344–353.
[9] K. Studer, C. Decker, E. Beck, R. Schwalm, Overcoming oxygen inhibition in UV-curing of acrylate coatings by carbon dioxide inerting, part I, Prog. Org. Coat. 48 (1) (2003) 92–100.
[10] K. Taki, R. Yamada, Comparison of the degree of shrinkage under air and nitrogen atmospheres by laser displacement sensor, J. Photopolym. Sci. Technol. 31 (4) (2018) 497–501.
[11] J. Zhou, X. Allonas, X. Liu, Fluorinated organozirconiums: Enhancement of overcoming oxygen inhibition in the UV-curing film, Prog. Org. Coat. 120 (2018) 228–233.
[12] N. Nagai, T. Matsunobe, T. Imai, Infrared analysis of depth profiles in UV-photochemical degradation of polymers, Polym. Degrad. Stab. 88 (2) (2005) 224–233.
[13] J. Huang, T. Yuan, X. Ye, L. Man, C. Zhou, Y. Hu, C. Zhang, Z. Yang, Study on the UV curing behavior of tung oil: mechanism, curing activity and film-forming property, Ind. Crop. Prod. 112 (2018) 61–69.
[14] J.W. Park, G.S. Shim, J.G. Lee, S.W. Jang, H.J. Kim, J.N. Choi, Evaluation of UV curing properties of mixture systems with differently sized monomers, Mater 11 (4) (2018).

[15] S. Matsui, H. Hiroshima, Y. Hirai, M. Nakagawa, Innovative UV nanoimprint lithography using a condensable alternative chlorofluorocarbon atmosphere, Microelectron. Eng. 133 (2015) 134–155.

[16] R. Bail, J.Y. Hong, B.D. Chin, Effect of a red-shifted benzotriazole UV absorber on curing depth and kinetics in visible light initiated photopolymer resins for 3D printing, J. Ind. Eng. Chem. 38 (2016) 141–145.

[17] Z. Jia, J. Choi, S. Park, Selection of UV-resins for nanostructured molds for thermal-NIL, Nanotechnology 29 (36) (2018), 365302.

[18] F. Saito, I. Nishiyama, T. Hyodo, An improved method for the measurement of adhesion energy by using a nano-cutting machine, Surf. Coat. Technol. 205 (2) (2010) 419–422.

[19] B. Son, M.-H. Ryou, J. Choi, T. Lee, H.K. Yu, J.H. Kim, Y.M. Lee, Measurement and analysis of adhesion property of lithium-ion battery electrodes with SAICAS, ACS Appl. Mater. Interfaces 6 (1) (2013) 526–531.

[20] K. Kim, S. Byun, I. Cho, M.-H. Ryou, Y.M. Lee, Three-dimensional adhesion map based on surface and interfacial cutting analysis system for predicting adhesion properties of composite electrodes, ACS Appl. Mater. Interfaces 8 (36) (2016) 23688–23695.

[21] N. NAGAI, Depth Profile Analysis by Infrared Spectroscopy, Analytical Sciences/Supplements Proceedings of IUPAC International Congress on Analytical Sciences 2001 (ICAS 2001), The Japan Society for Analytical Chemistry, 2002 i671–i674.

[22] J.-W. Park, Evaluation of Curing Shrinkage of the Photo-curable Material and Its Application for Photo-curable Adhesives, Seoul National University, 2016.

[23] C.B. Ruiz, L.D.B. Machado, J. Volponi, E.S. Pino, Oxygen inhibition and coating thickness effects on UV radiation curing of weatherfast clearcoats studied by photo-DSC, J. Therm. Anal. Calorim. 75 (2) (2004) 507–512.

[24] C.E. Corcione, M. Frigione, Factors influencing photo curing kinetics of novel UV-cured siloxane-modified acrylic coatings: oxygen inhibition and composition, Thermochim. Acta 534 (2012) 21–27.

[25] J.W. Park, S.J. Lee, H.W. Jung, H.S. Ahn, H.J. Kim, J.K. Cho, B. Kim, S. Shin, T.S. Hwang, Evaluation of soft adhesives containing dual-curable melamine-based compounds, Int. J. Adhes. Adhes. 70 (2016) 315–321.

[26] L-H. Lee, Fundamentals of Adhesion, Springer Science & Business Media 2013.

[27] K. Friedrich, Friction and Wear of Polymer Composites, Elsevier, 2012.